New Journal and we have not received input yet 25 (2021) 101034

Contents lists available at ScienceDirect

Thermal Science and Engineering Progress

journal homepage: www.sciencedirect.com/journal/thermal-science-and-engineering-progress

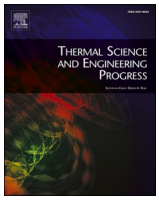

Investigation and prediction of ethylene Glycol based ZnO nanofluidic heat transfer versus magnetic effect by deep learning

Ahmet Beyzade Demirpolat [a,*], Muhammet Baykara [b]

[a] Department of Electronics and Automation, Vocational School of Arapgir, Turgut Ozal University, Malatya 44800, Turkey
[b] Department of Software Engineering, Faculty of Technology, Firat University, Elazig 23100, Turkey

ARTICLE INFO

Keywords:
Nanoparticles
Nanofluids
Heat transfer coefficient
Computational intelligence
Magnetic effect
Deep learning

ABSTRACT

In this study, ZnO (zinc oxide) nanoparticle production was performed. Heat transfer coefficients (h) were measured for Ethylene Glycol Based ZnO nanofluids that were produced using pure water, ethanol, and ethylene glycol materials. In the literature, this is the first study in which Nanofluid was produced and experimental results were estimated by using LSTM and CNN-LSTM deep learning models. The study graphs' show the relationship between heat transfer coefficients. Besides, Reynolds numbers were drawn and predictive models were created by using the LSTM and CNN-LSTM deep learning models for h values of nanofluids. In addition, the deep learning architecture that predicts the effects of the magnetic effect on the heat transfer coefficient has been introduced to the literature as an innovation. The results showed that the heat transfer coefficients can be estimated with the LSTM and CNN-LSTM deep learning model with an average error of 0.7342% and 0.2001% respectively. In addition, the relative error of the heat transfer coefficients as a result of the magnetic effect was determined as 0.02944 and 0.01701, respectively, with the same methods and model. Applying the magnetic effect to the system, an irregularity was observed in the flow and as a result of increased heat transfer, the friction on the pipe wall increased. The importance of the study is modeling the heat transfer coefficient values depending on the different pH values that were used during the synthesis of ZnO nanomaterial and observing the effects of the magnetic effect on the system.

Introduction

In our daily life, we encounter the flow in circular and non-circular pipes. The hot and cold water we use in our homes is pumped through the pipes. City water is distributed with an expensive pipe network. Oil and natural gas are transported by hundreds of kilometers of pipelines. The cooling water in the engine is transported to the pipes in the radiator which is cooled while flowing through the hoses by means of hoses. Most fluids, especially liquids, are transported by circular pipes [1]. Energy transfer through heat is a key process in several daily life applications and industrial processes. One of the most crucial daily life need is energy demand that is increasing day by day. Fossil fuel's actual energy sources are rapidly consumed. For this reason, it is very important to innovate existing energy conversion systems and to develop new methodologies for gaining more benefits from existing limited energy resources [2]. With the development of nanotechnology, we can produce nanomaterials that could be added to fluids to enhance their properties. There are many different techniques for producing nanoparticles such as chemical vapor condensation, microemulsion, hydrothermal technique, gas-phase production technique, and inert gas condensation technique [3]. By incorporating the nanoparticles into the working fluid, the performance of heat transfer is significantly improved [4]. Nanoparticles, nanofibres, nanotubes, and other nanomaterials are produced primarily as dry powder by physical methods or chemical methods. Then, these nano-sized powders are dispersed in water, the basic fluid. To stabilize the particles in the fluid and to obtain a homogenous distribution, the processes such as magnetic mixing, ultrasonic mixing, high shear mixing are applied [5].

Adding nanoparticles in the fluids changes the thermophysical properties of these nanofluids resulting in improve heat transfer, therefore the correct measurement of these nanofluid properties is important [6]. Many different studies have been carried out in the literature on this subject. Colangelo et al. produced different nanofluids in their study [6]. They stated that the low thermal conductivity fluids used in the production increase the thermal conductivity of the nanofluids they use. In 2001, Eastman et al. measured the thermal

* Corresponding author.
E-mail address: ahmetb.demirpolat@ozal.edu.tr (A.B. Demirpolat).

https://doi.org/10.1016/j.tsep.2021.101034
Received 5 April 2021; Received in revised form 4 August 2021; Accepted 5 August 2021
Available online 11 August 2021

Table 1
Literature summary of studies on heat transfer of nanofluids.

References	Basic fluid	Particles	Particle size	Volumetric ratio of particle(%)	Circular Pipe Dimensions	Flow regime, Reynolds Number	Result
Pak and Cho [14]	Water	g-Al_2O_3 TiO_2	13 nm 27 nm	1–3 1–3	1.066 cm diameter 480 cm length Brass Pipe	104 < Re < 205 (Laminar)	Increased volumetric rate of nanoparticles and the number of Re has increased heat transfer.
Xuan and Li [15]	Water	Cu	<100 nm	0.3,0.5,0.8,1, 1.2, 1.5, 2	10 mm diameter 800 cm length Brass Pipe	10000 < Re < 25000 (Turbulence)	Increased volumetric rate of nanoparticles and the value of the flow rate has increased heat transfer.
Xuan and Li [16]	Water	Cu	26 nm	0.5, 1, 1.5, 2	1.29 mm diameter Copper Pipe	200 < Re < 2000 (Laminar)	Heat transfer at the 2% volumetric ratio of Cu nanoparticle increased 39%.
Zhou [17]	Acetone	Cu	80-100nm	0.1–0.4	16 mm diameter 200 mm length Copper pipe	200<Re<1800 (Laminar)	The heat transfer coefficient increased with the increase in the percentageof nanoparticles (CuO).
Williams and friends [18]	Water	ZrO_2	46nm	0.9–3.6 0.2–0.9	1.27cm diameter 1.65 mm length Copper pipe	9000<Re<63000	The heat transfer coefficient increased with the increase in the percentage of nanoparticles (ZrO_2).
Sajadi and Kazemi [19]	Water	TiO_2	30nm	0.05,0.1,0.15, 0.20, 0.25	1.40mm diameter Copper Pipe	500< Re<3000 (Laminar)	The heat transfer coefficient increased with the increase in the percentageof nanoparticles (TiO_2).

conductivity of the nanofluids produced at concentrations between 0.01% and 3.0% and found that the hot oil, which is the basic fluid, exhibited much more thermal performance than water by using CuO, Al_2O_3, ZnO, and Cu particles [7]. Prajapati and Rohatgi used an ultrasonic vibration mixer in their work and, prepared ZnO-water nanofluids with a volume concentration ranging from 0.0001% to 0.1%. They also used the thermal properties analyzer to calculate the thermal conductivity of ZnO-water nanofluids. They achieved a maximum thermal conductivity value in a pressure range of 1–2.5 bar and a heat flow of 0–400 kW/m^2 at a constant mass flow rate of 400 kg/m^2. As a result, they showed that the heat transfer coefficient increased with increasing pressure and ZnO concentration [8].

The heat transfer applications depend on the thermophysical properties of nanofluids. Thermophysical properties are determined by different parameters such as specific heat capacity, viscosity, thermal conductivity, and heat transfer coefficients. The heat transferability of a nanofluid is well analyzed by the heat transfer coefficient [9]. Nguyen has studied the effect of particle size on the viscosity of the nanofluid with the composition of aluminum water. The study shows that the same results were obtained for particles with 36 and 47 nm in a 4% volumetric ratio. They also observed that the viscosity of the fluid increases with the increase in particle size [10]. Yadav and Sahu studied the effect of helical surface disc turbulators on the heat transfer properties of a double tube heat exchanger. They developed correlations for Nusselt number and thermal performance factor for Reynolds number varying between 3500 and 10.500 [11].

It is well known that solid metals have higher conductivity than fluids therefore the addition of solid nanoparticles into the fluids increases the thermal conductivity of the fluids [12]. Xie et al. have investigated the particle size effects on the thermal conductivity of the nanofluid by introducing the non-oxide ceramic nanofluid (SiC) of the particle size from 26 to 600 nm and aluminum oxide Al_2O_3 nanoparticles with the size range from 1.2 to 3.02 nm into the nanofluid [13].

In Table 1, studies in the literature on heat transfer enhancements of nanofluids are given. These studies are shown according to basic fluids, nanoparticle type, volumetric ratio, nanofluid transition pipe properties, flow regime, and Reynolds number.

In today's experimental studies, many data are obtained and necessary calculations are made on these data. Computational intelligence methods have been developed to facilitate data processing. A large number of data is easily processed with these methods. In this study, the modeling of the data obtained by applying the magnetic field effect of the heat transfer property of nanofluid by using two deep learning architectures (CNN and CNN-LSTM) that has been investigated. In the study, we synthesized ZnO nanoparticles of various particle sizes and Scanning Electron Microscopic (SEM) images were used to verify the size and morphology of these particles. These nanoparticles were used to prepare nanofluids by mixing them with water, ethanol, and ethylene glycol, and then a nanofluid was obtained, which was used in the experimental setup to determine the heat transfer coefficients of these fluids. A prediction model was created using LSTM and CNN algorithms for the heat transfer coefficients obtained for ZnO in the experimental setup where the magnetic field effect was applied. In these predictive models, the error values are analyzed and compared to find the best predictive model for the heat transfer properties of the nanofluid. In our study, the effect of magnetic field on heat transfer of nanofluids was investigated as an innovation, and the results obtained with the deep learning method, which was used for the first time in studies in this field, were predicted.

Materials and methods used in the study

In our research, the heat transfer coefficient values were determined experimentally by applying the magnetic field effect for various nanofluids prepared at different pH values. Based on these experimental data, different deep learning architectures such as LSTM and CNN-LSTM were used to estimate heat transfer coefficient values. In this section, detailed information and explanations about nanofluid production, uncertainty analysis, SEM analysis, heat transfer in nanofluids and deep learning architecture and modeling data are given.

Production of nanofluids and obtaining heat transfer coefficients with the experimental setup

In the production of nanomaterial, the Chemical Mixing method, which is a method of converting the substance into an insoluble form or changing the composition of the solvent to reduce its solubility in the substance, is used [14]. In ZnO particle production, 2.20 g (0.01 mol) Zinc Acetate was dissolved in 50 ml ethanol solvent for 15 min using the magnetic stirrer. After that 4 g (0.1 mol) NaOH (Sodium Hydroxide) and

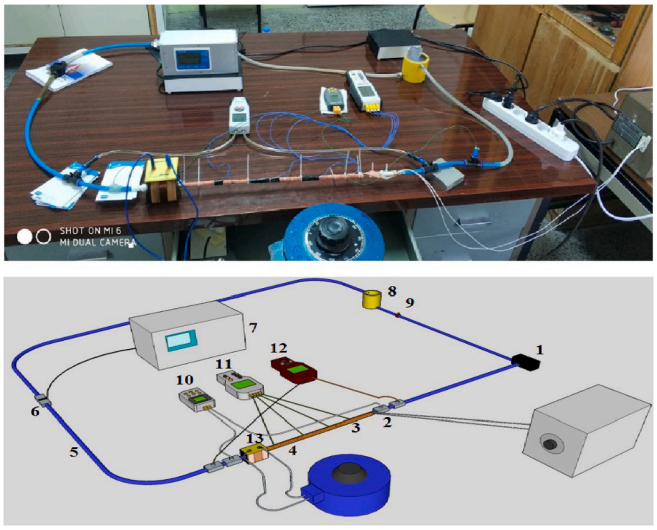

Fig. 1. The experimental setup.

100 ml of pure water were added to the mixture and further dissolved by using an ultrasonic bath for a time period of 15 min. The dissolved Zinc Acetate and NaOH mixtures were mixed together and stirred using a magnetic stirrer for an hour. The pH ratios for different solutions were adjusted by adding an appropriate amount of ammonia solution into the mixtures.

The nanoparticles were obtained by precipitating the mixture for approximately 20 h. The precipitated particles were filtered and rinsed with pure water and ethanol several times to remove any impurities from the solution. The washed powder was then dried at 55 °C to remove any remaining moisture from it. The white nanoparticle powder was heat-treated at 460 °C for 1 h. Finally, the successful production of ZnO nanoparticles was confirmed through the SEM images.

For nanofluid production, the Two-Step method most commonly used in the literature was applied [15]. In the Two-Step method, nanoparticles, nanofibers, nanotubes, and other nanomaterials were first produced as particles in dry powder form by using chemical or physical methods. As a second step, these nano-sized powders were dispersed in the base fluid. Ultrasonic mixing was performed in order to obtain a homogenous distribution by stabilizing the particles in this mixture [16]. After the successful production of the ZnO nanoparticles, the next step is to prepare the nanofluid from the obtained nanoparticles. For this purpose, the various amounts of nanopowder (0.1%, 0.2%, and 0.3%) were mixed with a solution of 56.9% Pure Water, 28.9% Ethylene Glycol and 14.2% Ethanol and were stirred 50 min ultrasonically to get homogenous and stable nanofluid.

The formed nanofluids are ready for use in the experimental setup, but before using these nanofluids, the density of the nanofluids was determined. The experiments were performed for the produced nanofluids and five different Reynold values were calculated. In our experiment, the temperature values of the fluid were measured regularly with 5 min time interval. The temperature readings were taken by attaching four thermocouples placed equidistance from each other at the pipe surface and the readings were started after the stable temperature was obtained. From these experimental values, the heat conduction coefficient and heat transfer coefficients were calculated.

Fig. 1 shows the experimental setup for the calculation of the heat transfer coefficient. The figure shows a control valve that is used to control the flow rate of the nanofluid. The temperature readings were measured to determine the heat transfer properties of the fluid from the copper pipe surface with laminar fluid flow and in order to reduce the experimental error, four thermocouples were placed on the pipe. By using the thermometers at both ends, the inlet and outlet temperatures of the nanofluid were measured. The flow meter shows the volumetric flow rate of the nanofluid.

1-Fluid pump, 2- T Connection, 3-Heat Tape, 4-Copper pipe, 5-Plastic pipe, 6- Electronic flow meter sensor, 7-Electronic flow meter, 8-Fluid reservoir, 9-Flow regulating valve, 10-Fluid Thermometer, 11-Thermocouple, 12-Manometer, and 13- Coil

Table 2
Uncertainty values.

Parameter	Uncertainty results (%)
Temperature measurements	±%3.2
Mass and time measurements	±%1.1
Uncertainty resulting from differences in pipe length	±%1
Uncertainty caused by differences in pipe diameter	±%1
Uncertainty of Physical Properties (Viscosity and Density)	±%1
The uncertainty in the Reynolds number	±%2.75
Uncertainty of heat transfer coefficient	±%4.55

Uncertainty analysis

The uncertainty analysis was performed for the measurements and for the calculations we made. Temperature and volumetric flow measurements were performed in the experimental study. Reynolds number (Re) and heat transfer coefficient (h) were calculated from these measurements. The uncertainty analysis values of the measurements used for the calculations which were based on the method determined by Kline and McClintock [17]. In measuring the value of a parameter, the total error calculation can be calculated as in Eq. (1) by taking into account the errors caused by fixed errors, random errors, and manufacturing errors [18].

$$w_x = [(x_1)^2 + (x_2)^2 + \ldots\ldots + (x_\infty^2)]^{1/2} \quad (1)$$

The uncertainty analysis calculated for various parameters is shown in Table 2.

Scanning electron microscope (SEM) analysis

The SEM images are typically taken by focusing a beam of electrons having energy from 200 to 300 eV to 100 keV. The electron beam is focused by using electromagnetic lenses onto the target surface and interacts with the surface. The secondary electrons emerging from the depth of about 10 nm from the sample surface with 50 eV typical energies are collected to form an image [19]. The SEM images were taken by using the JEOL SM-7001F Field Emission SEM. The images in Fig. 2 show the morphology of different nanoparticles obtained using the participation method at different pH values.

According to the electron microscopic images, it is clear from morphology and the dimensions of these particles that the ZnO nanoparticles were formed successfully. The particles with a size ranging equal to or <100 nm are considered nanoscale materials and thus forms the basis of nanotechnology [20]. ZnO nanofluids with different crystallite sizes (164, 60.9, 33,47.8, 121 and 123 nm) have been prepared by chemical route using a different solvent. SEM image shows that 164 nm crystallite size particles are of rod shape whereas 60.9 nm crystallite size are elliptical shape particles. 33 and 47.8 nm size particles are almost spherical aggregates whereas 121 and 123 nm crystallite size particles show the mixed shapes of spherical as well as elongated rod shape particles. The change in morphology is due to the different reaction rates of solvents used in the reaction to produce ZnO nanoparticles [21].

The morphological structure of our materials, i.e. the size of the nanoparticles we produce to prepare the nanofluids, is effective on heat transfer of nanofluids, heat conduction, viscosity, and many thermophysical properties. The change in the morphology of the ZnO nanoparticles is due to its pH value. When the pH value increases, the heat transfer decreases and when the pH value decreases, the round grains turn into a rod shape.

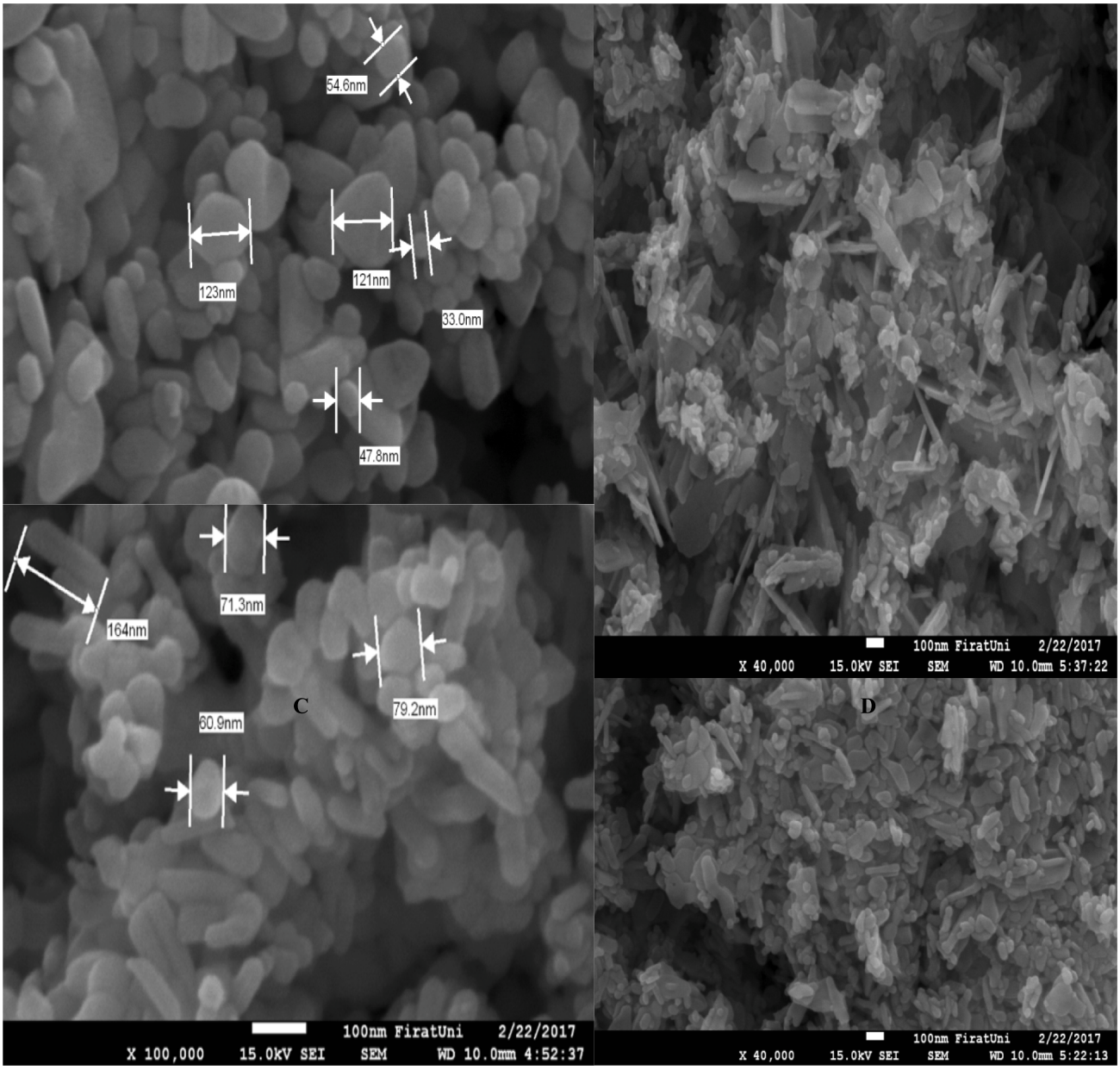

Fig. 2. SEM image of ZnO (A: at pH 7,7, B: at pH 8,7, C: at pH 8,5, D: at pH 9,9).

Heat transfer in nanofluids

The energy is transferred between different environments and objects which are at different temperatures. The transfer of energy is referred to as energy transmission when it happens between the stationary solid or fluid, whereas the term transport is utilized when the heat transfer occurs between the surfaces and fluids in motion at different temperatures. The surfaces emit their energy in the form of electromagnetic waves at finite temperature. The heat exchange between the surfaces without any direct contact is called radiation [22]. Effective thermal conductivity not only depends on the inherited thermal conductivity value of the materials but also on the porosity or volume fraction of the medium. The studies have shown in both laminar and turbulent flow conditions, the heat transfer coefficient of nanofluids and the thermal conductivity value is greater than the heat transfer properties of pure water.

Newton described the basic law of cooling for the transport of heat energy before Fourier's transmission law of energy. The heat transfer coefficient can be calculated from fundamental Eq. (2) which is given below.

$$Q = hA\left(T_w - T_f\right) \tag{2}$$

In this relationship, Q represents the amount of heat energy transfer between the walls and liquid flowing through the copper tube and A is the common surface area between them. Whereas T_w is the average surface temperature and T_f is the average temperature of both ends (in & out) of the copper tubing [23].

The Reynolds number at which the flow becomes turbulent is called the Critical Reynolds number Recr. The value of the Critical Reynolds number varies for different geometries and flow conditions. The generally accepted value of the Critical Reynolds number for internal flow in a circular pipe is $Re_{cr} = 2300$. We want to know the exact values of the Reynolds number for laminar, transitional and turbulent flows. But in practice it is not so easy to determine the exact values. In most

practical applications the flow in circular pipes is laminar for Re ≤ 2300. For Re ≥ 4000 the flow is turbulent and at Reynolds number values between these two values (2300 ≤ Re ≤ 4000) the flow becomes a transitional flow. In circular pipes; Nusselt number is constant in laminar flow, constant surface heat flux (q_s = constant), and fully developed flow conditions; It does not depend on Reynolds or Prandtl numbers [23]. Considering this situation in the literature, Reynolds number was made between 800 and 2300 in our study. The reason for this is to facilitate the determination of the heat transfer coefficient when needed.

$$Nu = \frac{hD}{k} = 4.36 \tag{3}$$

The magnetic field is calculated using the magnetic field density β (Wb/m^2) applied along the pipe, magnetic field intensity H (A/m), number of turns in N coil, I current, ℓ conductor length and μ magnetic permeability coefficients. The formula in Equation (4) is used for calculation.

$$H = \frac{NI}{\ell}, \beta = \mu H \tag{4}$$

Modeling data with deep learning architecture

The Deep Learning Architecture (DLA) is a subcategory of Machine Learning (ML). A deep neural network is a different neural network model with neurons having a lot of parameters and layers in between the layer of input and output. Deep learning is considered as the modern architecture of neural networks. DLA provides automatic learning of features. It also provides feature representation in a hierarchical manner at different levels. This powerful learning process makes DLA more robust and reliable, unlike machine learning methods. In short, DLA is used with high performance for feature extraction and alteration process. In DLA, simple processing procedures of input data and learning easy features are performed in the initial layers. The outputs of the initial layers are given as input for the upper layers that can learn more complex features. Therefore, deep learning is more suitable for complex problems with large data. Areas such as image classification, video analysis, speech recognition and natural language learning can be given as examples of the usage areas of DLA [24–26].

In this study, a prediction model has been developed for the calculated heat transfer coefficient of the nanofluid by using convolutional neural networks in the first phase and convolutional neural network and LSTM architecture in the second phase. According to the prediction accuracy, it was observed that the approach in the second phase was more successful than the model in the first phase. To the best of our knowledge, the developed model in this study is the first on this subject in the literature.

Long-short term memory

Long-Short Term Memory (LSTM) is a more developed version of recurrent neural networks (RNNs). RNN architectures have an approach based on previous knowledge usage. Therefore, RNNs do not only handle the input instances that have entered the network, but also the input instances within the input previously. In traditional neural networks, input data is given to the network independently. However, the situation is different in RNN architecture. Besides, in RNNs, the output of each data in the array is calculated with previous values. RNNs are a class of neural networks in which connections between units form a directed loop [27]. Recurrent neural networks, unlike feedforward neural networks, can use input memory to process random input sequences [28]. The main idea here is to use sequential information. However, the vanishing gradient problem arises in RNN architectures. when the gap between contexts increases, it becomes difficult to use information from the past, which causes this problem to arise.

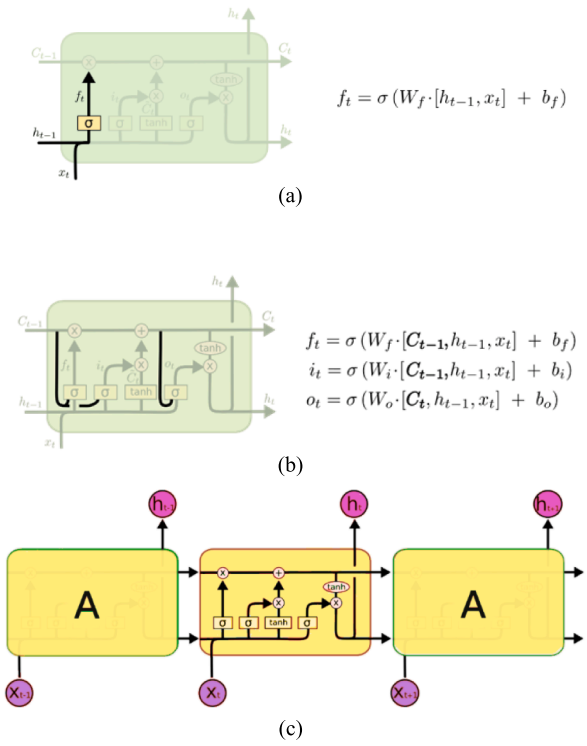

Fig. 3. General structure of LSTM architecture. (a) forget gate, (b) peephole, and (c) LSTM block.

Therefore, a modified LSTM has been proposed to solve this problem [29]. Basically, LSTM architecture consists of three gates, namely input, forget and output gate. The cell remembers values in arbitrary time intervals and these three gates adjust the flow of information in and out of the cell. The output of the block is repeatedly linked to the entrance of the block and all its gates. LSTM networks are well suited to classify, process and make predictions on data such as time series. A general structure of the LSTM architecture is given in Fig. 3.

LSTM deep learning architecture is used in many areas based on letters. Speech recognition [30], text generation [31], music composition [32] can be given as examples to these areas. However, in addition to these areas, LSTM architecture is used in many areas such as biomedical signal processing [33,34], bioinformatics [35,36] and cyber-attack detection [37]. The accuracy rate of the LSTM deep learning architecture in the classification area also guided the prediction studies. There are studies such as forecasting tourism flow with LSTM deep learning model [38], forecasting stock prices [39], forecasting e-commerce time series [40], forecasting natural gas prices and movement [41]. When these studies were examined in detail, it was seen that LSTM performed an effective estimating process. Due to this prediction success of the LSTM method in the literature, it was thought to be useful to develop an estimation model with LSTM for heat transfer coefficient estimation of nanofluids containing ZnO. In this study, the LSTM deep learning model was used, the heat transfer change of ZnO nanofluids and the heat transfer changes due to the magnetic field were estimated and compared with the experimental results. LSTM deep learning model was modeled as sixteen inputs and one output in the system. Reynolds number (Re), fluid volume (ml), time (sec), flow rate (lt/sec), velocity (m/sec), surface heat flux (ya), pipe diameter (m), heat for the fluid (T_{in}, T_{out}, T_{avg1}, T_1, T_2, T_3, T_4, T_{avg2}), and Conduction coefficient (k) used in the experiments are taken as input information. The heat transfer coefficient (h) of nanofluids was used as output information. The designed LSTM deep learning model is given in Fig. 4.

As can be understood from Fig. 4, the designed LSTM model consists of an input layer, two LSTM layers and one output layer. The parameters

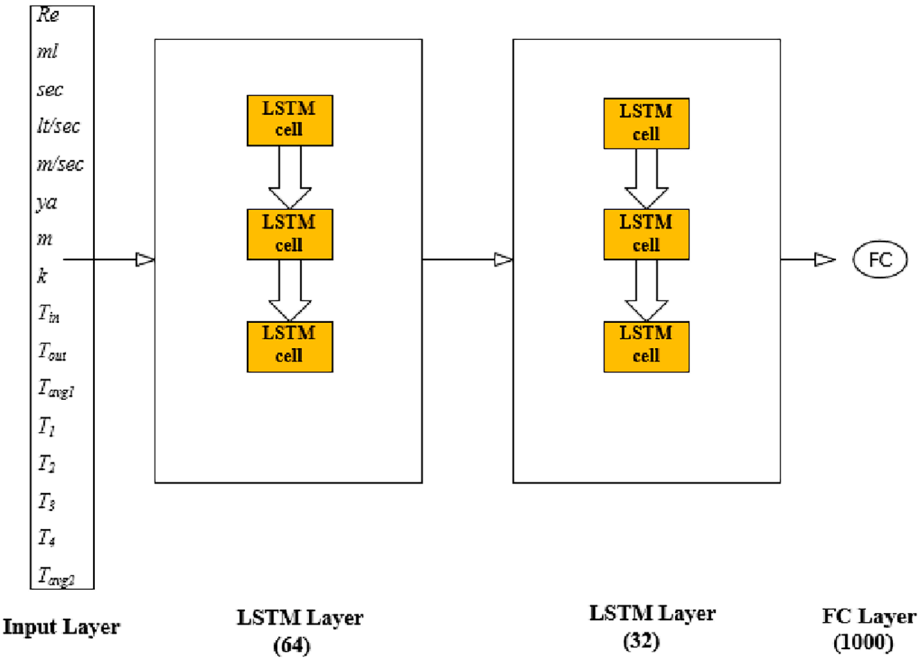

Fig. 4. Structure of the designed LSTM model.

of the designed LSTM model were determined by trial and error approach and the parameters that perform the best estimation process were selected. The parameters can be given as follows;

- A total of 16 inputs were used in the input layer.
- Then, the LSTM layer was defined in the second layer and 64 LSTM units were used in total. ReLU was preferred as the activation function.
- In the 3rd layer, the LSTM layer was evaluated again and 32 LSTM units were preferred this time. ReLU was used again as the activation function in this layer.
- In the last layer, a fully connected layer consisting of 1000 neurons was designed and the estimation process was performed. A total of 1000 estimation procedures were performed using 1000 neurons, and the estimation result was determined by considering the average value.
- The Adam function was used as an optimization function. Here, the learning rate was chosen as 0.01.
- The loss of the system was calculated with the mean square error.
- All these operations were carried out with 1000 epoch values.

Convolutional neural network with LSTM model

CNN is a deep learning algorithm that is often used in image processing and takes images as input. CNN, which captures the features in images with different operations and classifies them, consists of different layers. These layers are input, convolutional, pooling, fully-connected, and output layers. Images are brought into a state that can enter the deep learning model by passing through these layers. Since we are dealing with unstructured data while creating CNN models, there is not much effort in data pre-processing according to classical machine learning algorithms.

In the CNN algorithm, information that is in the input layer is processed with feature extraction and transformation in the convolution and pooling layers. The local information of the pooling and convolution layers here, are integrated by the fully-connected layers and mapped to the output signals via the output layer. CNN algorithm is used in many fields such as natural language processing and biomedical, especially image and sound processing [42]. A general working diagram showing

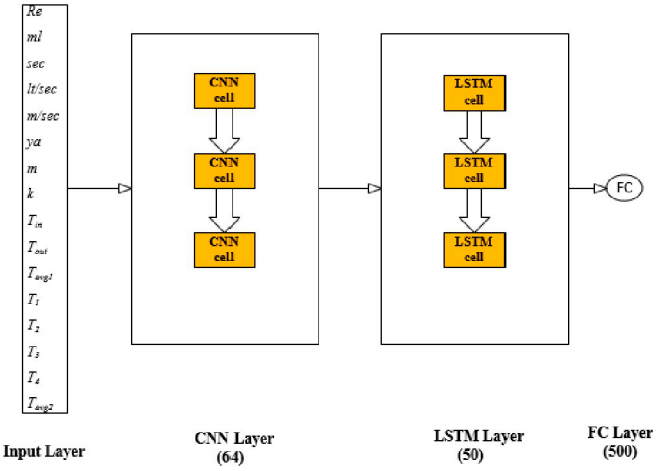

Fig. 5. Structure of the designed CNN-LSTM model.

the layers of the CNN algorithm is given in Fig. 5.

As can be seen from Fig. 5, the designed CNN-LSTM model consists of an input layer, a CNN layer, an LSTM layer, and an output layer. The parameters of the designed CNN - LSTM model were determined by trial and error approach and the parameters that perform the best estimation process were selected. The parameters can be given as follows;

- There are a total of 16 entrances in the entry layer.
- In the second layer, the CNN layer is defined and a total of 64 CNN units are used. ReLU was preferred as the activation function. Max-pooling and flatten structures were used. With max-pooling, it is aimed to reduce the number of calculations and use smaller outputs containing enough information for the neural network to make the right decision. It was aimed to prepare the data with Flatten and 50 LSTM units were used and ReLU was chosen as the activation function.
- In the last layer, a fully connected layer consisting of 500 neurons was designed and the estimation process was performed. A total of 500 estimation procedures were performed using 500 neurons, and

Table 3
The Criteria of Accuracy and Formulas.

The Criteria	Formulas	Parameters
RMSE	$\sqrt{\frac{(P1-A1)^2+.....+(Pn-An)^2}{n}}$	P: Predicted result A: Actual result n: Total Estimated result
RAE	$\frac{\lvert P1-A1\rvert+.....+\lvert Pn-An\rvert}{\lvert A1-A'\rvert+.....+\lvert An-A'\rvert}$	P: Predicted result A:Actual result A': Average of Actual results
RRAE	$\sqrt{\frac{(P1-A1)^2+.....+(Pn-An)^2}{(\lvert A1-A'\rvert)^2+.....+(An-A')^2}}$	P: Predicted result A: Actual result A': Average of Actual results

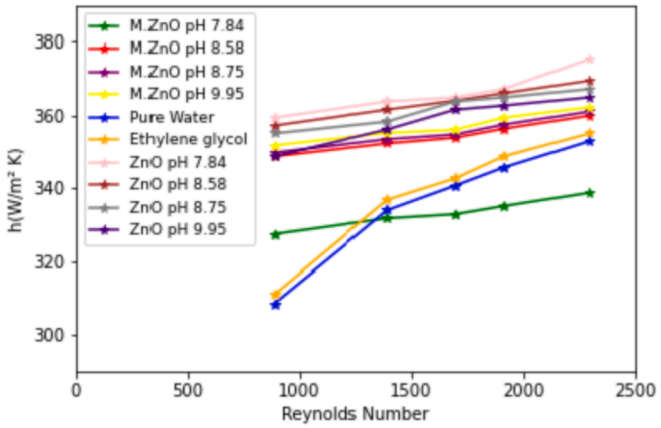

Fig. 6. Evaluation of the change of heat transfer coefficient values obtained for ZnO pH values according to Reynolds number.

the estimation result was determined by considering the average value.

- The Adam function was used as an optimization function. The learning rate was chosen as 0.01.
- The loss of the system was calculated with the mean square error.
- All these operations were carried out with 500 epoch values.

The main purpose of our study is to estimate the heat transfer coefficients according to different Reynolds values rather than classification using the deep learning model. Since no classification process was performed in our research, the data were not separated as training and test data. Hence accuracy, precision, recall, ROC, etc. evaluation matrices were not calculated. In addition, no cross-validation was performed in the study. Because operations such as cross-validation, separation of training, and test data are the methods used in the classification process. Similar approaches were used in other studies in the literature, and cross-validation, holdout-validation, etc. were not used in these studies [43–45].

The formula and parameters of root mean squared error (RMSE), relative absolute error (RAE) and root relative absolute error (RRAE) analyzes were used to determine the accuracy rates of computational intelligence methods which are shown in Table 3.

Results and discussion

In this study, the heat transfer coefficient of ethylene glycol-based ZnO nanofluids that were obtained at various pH values was calculated and it was found that the heat transfer coefficient value for various prepared nanofluids increased with Reynold's number between 800 and 2300. Then, the magnetic field effect on nanofluids was investigated by creating a magnetic field in the experimental setup. Fig. 6 shows the inverse relationship between the heat transfer coefficient and the pH value. When producing nanomaterials, a mixture of 25% NH3 and 75% water is used to adjust the pH during the production of ZnO nanoparticles. As a result, the specific heat of the liquid is adversely affected as the pH level rises. As can be seen in Fig. 6, it has been observed that the heat transfer increases with the increase of the pH rate as a result of the magnetic field effect. The reason for this, that can be said as the decrease in the nanoparticle ratio in the fluid with the increase of pH, the specific heat of the liquid is adversely affected as the pH level increases, and the flow is seen closer to the pipe wall where the flow becomes irregular with the effect of the magnetic field.

When Fig. 6 is examined; It was concluded that the heat transfer was negatively affected by the effect of the magnetic field, because the tube type and nanoparticle type were effective. The error rates of predicted LSTM and CNN-LSTM models that were created for heat transfer coefficients of ZnO nanofluids were shown in Table 4.

When Fig. 7 is examined, it is observed that there is no significant change in heat transfer as a result of the magnetic field effect with the increase of the nanoparticle ratio. The error rates of predicted LSTM and CNN-LSTM models that were created for heat transfer coefficients of ZnO heat transfer coefficients were shown in Table 5.

Recently, computational intelligence methods have been used in almost every field. Obtaining a predictive model of a situation in different methods is important for features such as design, innovation, production, and development. There are many valuable studies in the literature in order to create a predictive model of thermophysical properties of nanofluids using computational intelligence methods. In the literature, to create a predictive model of various nanofluids thermophysical properties different studies have been performed by using support vector regression (SVR), multi-layer perceptron (MLP), genetic algorithm-radial base function (GA-RBF), artificial neural network (ANN), decision tree (DT) and support vector machine (SVM). These studies are shown in Table 6.

Table 4
Error rates.

Deep learning algorithms	RMSE	RAE	RRAE
LSTM	0.7342	0.2940	0.2606
CNN-LSTM	0.2001	0.0621	0.0710

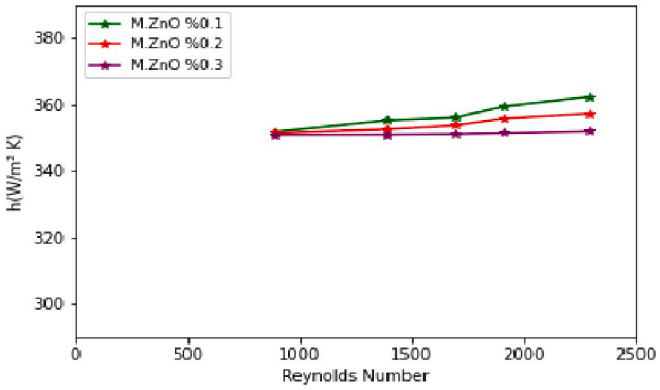

Fig. 7. Investigation of the heat transfer coefficient change as a result of magnetic field effect by increasing the ZnO nanoparticle ratio according to Reynolds number.

Table 5
The error rates are the result of the ZnO heat transfer coefficients obtained as a result of the magnetic field effect.

Deep learning algorithms	*RMSE*	*RAE*	*RRAE*
LSTM	0.02944	0.08861	0.09694
CNN-LSTM	0.01701	0.04740	0.05600

Table 6
Prediction models of thermophysical properties of nanofluids in the literature.

Nanofluids	Thermo-physical properties	Number of Data	Method	Error Analysis	Error Analysis Result	Reference
Al_2O_3, TiO_2 ,CuO, SiO_2	Heat transfer coefficient	274	SVR	RMSE	1.11	(Alade et al. 2018) [46].
Al_2O_3, SiO_2, TiO_2, CuO-water	Viscosity	3144	MLP	RMSE	0.1	(Hemmati-Sarapardeh et al. 2019) [47].
TiO_2 / SAE 50 nano-lubricant	Viscosity	174	GA-RBF	RMSE	0.58	(Esfe et al.2018) [48].
MWCNTs/ water	Viscosity	268	ANN	MSE	0.28	(Afrand et al.2016) [49].
Al_2O_3/EG	Heat transfer coefficient	154	SVM	MSE	$8.6x\ 10^{-5}$	(Ahmadi et al. 2019) [50].
Fe_2O_3/water	Heat transfer coefficient	84	MLP	RMSE	0.348	(Ahmadi et al. 2018) [51].

Table 7
Change of heat transfer values (Experimental).

Reynolds	ZnO pH:7.8	ZnO pH:8.5	ZnO pH:8.7	ZnO pH:9.9	33% Ethylene Glycol + 67% Pure Water	Pure Water
	Heat transfer coefficient (h,W/m^{2}K)					
880	359.42	357.24	355.11	348.79	311.05	308.61
1385	363.86	361.63	358.33	356.16	336.83	333.97
1614	364.98	364.12	363.86	361.63	342.70	340.72
1957	367.26	366.12	364.98	362.74	348.79	345.72
2240	375.45	369.56	367.26	364.98	355.11	352.96

Table 6 shows the nanofluids type, thermophysical properties, the number of data, the predictive method, the type of error analysis and the results of the error analysis. It shows the data from some of the previous studies and the error analysis along with the methods used for the computation. The results of RMSE error analysis for our studies to estimate the heat coefficient have less error compare to these studies. The change in the heat transfer of nanofluids containing ZnO with pH and Reynolds values is shown in Table 7. These results are obtained as experimental results. The heat transfer values according to the Reynolds number of ZnO nanofluids at different pH after the effect of magnetic field is applied to the system are given in Table 8.

According to Table 9, heat transfer increased as Reynolds value increased, and heat transfer decreased as pH increased. Table 9 shows the estimated results obtained according to the LSTM deep learning architecture given in Fig. 4. These results show the direct result of the codes generated in the Python programming language. There is no margin of error. Considering the deviations in the experiment, it can be assumed that the results here are satisfactory.

According to Table 10, heat transfer increased as the Reynolds value increased, and as a result of the magnetic field effect, it was observed that the heat transfer increased as the pH increased. Table 10 shows the estimated results obtained according to the LSTM deep learning architecture given in Fig. 4. These results show the direct result of the codes generated in the Python programming language. There is no margin of

Table 8
Change of heat transfer values (Experimental) for heat transfer values obtained as a result of ZnO magnetic field effect.

Reynolds	ZnO pH: 7.8	ZnO pH:8.5	ZnO pH:8.7	ZnO pH:9.9 %0.1	ZnO pH:9.9 %0.2	ZnO pH:9.9 %0.3	33% Ethylene Glycol + 67% Pure Water	Pure Water
	Heat transfer coefficient (h,W/m^{2}K)							
880	327.47	348.78	349.81	351.80	351.49	350.86	311.05	308.61
1385	331.76	352.33	353.43	355.26	352.62	350.92	336.82	333.96
1614	332.88	353.90	354.82	356.16	353.76	351.13	342.70	340.72
1957	335.12	356.37	357.53	359.42	355.83	351.49	348.78	345.71
2240	338.76	359.96	361.45	362.29	357.24	351.90	355.08	352.96

Table 9
Change of heat transfer values (Estimated with LSTM).

Re	ZnO pH:7.8	ZnO pH:8.5	ZnO pH:8.7	ZnO pH:9.9	33% Ethylene Glycol + 67% Pure Water	Pure Water
	Heat transfer coefficient (h,W/m^{2}K)					
880	366.23	357.32	357.22	341.41	310.53	316.75
1385	368.19	357.78	361.43	349.31	340.49	338.53
1614	368.34	366.53	367.99	365.71	340.81	342.65
1957	365.21	368.82	362.73	362.37	354.88	344.10
2240	374.54	369.85	369.97	369.78	352.44	358.90

Table 10
Change of heat transfer values (Estimated with LSTM) according to the magnetic field effect.

Re	ZnO pH: 7.8	ZnO pH:8.5	ZnO 8.7	ZnO pH:9.9 %0.1	ZnO pH:9.9 %0.2	ZnO pH:9.9 %0.3	33% Ethylene Glycol + 67% Pure Water	Pure Water
	Heat transfer Coefficient (h,W/m^{2}K)							
880	325.71	346.75	351.52	351.83	351.47	349.67	311.22	308.62
1385	331.10	352.45	355.63	355.23	352.62	352.79	336.78	334.59
1614	332.89	353.48	354.92	355.77	351.99	352.69	340.57	342.92
1957	335.10	356.70	357.56	359.54	355.78	353.52	346.52	345.74
2240	337.68	358.01	360.96	364.15	357.41	352.67	355.11	353.03

Table 11
Change of heat transfer values (Estimated with CNN-LSTM).

Re	ZnO pH:7.8	ZnO pH:8.5	ZnO pH:8.7	ZnO pH:9.9	33% Ethylene Glycol + 67% Pure Water	Pure Water
	Heat transfer Coefficient (h,W/m^{2}K)					
880	360.55	357.29	354.01	352.611	311.20	308.97
1385	363.95	361.80	358.48	355.99	338.95	334.39
1614	366.62	363.98	363.59	361.33	341.19	340.66
1957	368.02	366.32	364.63	362.74	348.09	344.36
2240	377.48	369.64	367.97	364.74	355.64	352.15

Table 12
Change of heat transfer values (Estimated with CNN + LSTM) according to the magnetic field effect.

Re	ZnO pH: 7.8	ZnO pH:8.5	ZnO pH:8.7	ZnO pH:9.9 %0.1	ZnO pH:9.9 %0.2	ZnO pH:9.9 %0.3	33% Ethylene Glycol + 67% Pure Water	Pure Water
	Heat transfer coefficient(h,W/m^{2}K)							
880	327.83	348.66	349.99	349.62	351.29	350.18	311.99	308.49
1385	331.50	352.29	353.51	356.83	352.84	350.67	336.83	333.68
1614	332.98	354.74	353.58	356.29	354.64	352.34	344.21	340.59
1957	335.14	356.34	357.58	359.23	355.65	351.46	348.12	345.77
2240	338.87	359.05	361.06	362.26	357.87	352.70	354.78	352.88

Table 13
Relative errors obtained with the LSTM deep learning model.

Re	ZnO pH:7.8	ZnO pH:8.5	ZnO pH:8.7	ZnO pH:9.9	33% Ethylene Glycol + 67% Pure Water	Pure Water
	Heat transfer coefficient (h,W/m^{2}K)					
880	1.8947	0.0225	0.6020	2.1128	0.1667	2.6409
1385	1.1927	1.0564	0.8689	1.9249	1.0888	1.3673
1614	0.9209	0.6726	1.1381	1.1290	0.5538	0.5664
1957	0.5569	0.7414	0.6153	0.1011	1.7489	0.4897
2240	0.2406	0.0939	0.7404	1.3163	0.7414	1.6829

Table 15
Relative errors obtained with the CNN-LSTM deep learning model.

Re	ZnO pH:7.8	ZnO pH:8.5	ZnO pH:8.7	ZnO pH:9.9	33% Ethylene Glycol + 67% Pure Water	Pure Water
	Heat transfer coefficient (h,W/m^{2}K)					
880	0.3144	0.0144	0.3023	1.0984	0.0482	0.1196
1385	0.0259	0.0563	0.0426	0.0480	0.6336	0.1290
1614	0.4499	0.0267	0.0720	0.0800	0.4422	0.0166
1957	0.2097	0.0559	0.0972	0.0016	0.1975	0.3906
2240	0.5432	0.0370	0.1945	0.0665	0.1576	0.2288

error. Given the deviations in the experiment, it can be assumed that the results here are satisfactory.

Tables 11 and 12 shows the estimated results obtained according to the CNN-LSTM deep learning architecture given in Fig. 5. These results show the direct result of the codes generated in the Python programming language. There is no margin of error. Considering the deviations in the experiment, it can be assumed that the results here are satisfactory. The results are almost 0% inaccurate and match the actual values.

The relative errors of the estimation results and experimental results obtained with the LSTM model are given in Tables 13 and 14. The relative errors of the estimation results and experimental results obtained with the CNN-LSTM model are given in Tables 15 and 16. There is a margin of error of approximately ± 4.5 in the results obtained with the experimental results. When the experimental results were reflected in this margin of error, it was seen that the difference between the estimated results and the experimental results almost %0. Because the biggest error with LSTM is 2.6409% and with CNN-LSTM the biggest error is 1.0984%. Considering the margin of error in the experimental values, it is clear that the predictive results are extremely successful.

Figs. 8–10 shows a comparison between the h values estimated by computational modelling and the values obtained from experimental study. Figs. 8–10 shows the actual and predictive values of the heat transfer coefficient (h) values. The 4 different increase distributions in the figures indicate the h value, which varies according to the Reynolds number calculated at 4 different pH values (See Figs 11–13).

Both the actual and predictive values of heat coefficient are shown in Figs 11–13, the graphs show that predictive values using LSTM and CNN-LSTM algorithm are very close to the actual values. This result can also be confirmed through the error analysis given in Tables 13 and 15. The CNN-LSTM algorithm predicts more accurately and its value of RMSE error analysis is less than the results achieved by ML methods. According to Tables 13 and 15, the CNN-LSTM method estimates with a 73% higher accuracy rate compared to the LSTM method.

Conclusions

In this work, the ZnO nanoparticles were produced successfully as shown through the SEM images analyses. The nanofluid was obtained by adding pure water, ethanol and ethylene glycol into the produced nanoparticles and the heat transfer coefficients were calculated. As the Reynolds number increased, the heat transfer coefficient of nanofulids increased in accordance with the calculations. The results showed that the heat transfer coefficients can be estimated with the LSTM and CNN-LSTM deep learning model with an average error of 0.7342% and 0.2001% respectively. In addition, the relative error of the heat transfer coefficients as a result of the magnetic effect was determined as 0.02944 and 0.01701, respectively, with the same methods and model. As a result, with the increase of the pH value of the nanofluids produced by adding ZnO nanoparticles, the heat transfer coefficient decreased. With the application of the magnetic effect to the system, irregularity was observed in the flow and the friction on the pipe wall increased, resulting in increased heat transfer. The increase of nanoparticle ratio, it has been observed that there is no significant heat transfer increase as a result of magnetic effect. This study is important in terms of modeling the heat transfer coefficient values depending on the different pH values used during the synthesis of ZnO nanomaterial and observing the effects of the magnetic effect on the system. In addition, LSTM deep learning and CNN-LSTM deep learning models were used for the first time with this study and a deep learning model was developed for heat transfer exchange of nanofluids. Based on the results obtained, it has beenrevealed that the type of nanofluid and the material forming the system is important, especially in systems where the magnetic field effect is used

Table 14
Relative errors obtained with the LSTM deep learning model according to the magnetic field effect.

Re	ZnO pH: 7.8	ZnO pH:8.5	ZnO 8.7	ZnO pH:9.9 %0.1	ZnO pH:9.9 %0.2	ZnO pH:9.9 %0.3	33% Ethylene Glycol + 67% Pure Water	Pure Water
	Heat transfer coefficient (h,W/m^{2}K)							
880	0.5370	0.5817	0.4857	0.0087	0.0063	0.3401	0.0557	0.0059
1385	0.2117	0.0353	0.6046	0.0075	0.0008	0.5356	0.0121	0.1888
1614	0.0041	0.1181	0.0146	0.1085	0.4984	0.4353	0.6203	0.6457
1957	0.0051	0.0915	0.003	0.0323	0.0146	0.5788	0.6475	0.0089
2240	0.3205	0.5432	0.0302	0.5122	0.3271	0.2196	0.0057	0.0190

Table 16
Relative errors obtained with the CNN + LSTM deep learning model according to the magnetic field effect.

Re	ZnO pH: 7.8	ZnO pH:8.5	ZnO pH:8.7	ZnO pH:9.9 %0.1	ZnO pH:9.9 %0.2	ZnO pH:9.9 %0.3	33% Ethylene Glycol + 67% Pure Water	Pure Water
	Heat transfer coefficient (h,W/m^{2}K)							
880	0.1100	0.0334	0.0485	0.6198	0.0571	0.1940	0.3049	0.0367
1385	0.0778	0.0112	0.0038	0.4430	0.0634	0.0702	0.0023	0.0844
1614	0.0289	0.2365	0.3644	0.0372	0.2490	0.3451	0.4415	0.0371
1957	0.0063	0.0085	0.0052	0.0527	0.0499	0.0081	0.1904	0.0177
2240	0.0319	0.2540	0.0016	0.0078	0.1767	0.2263	0.0837	0.0228

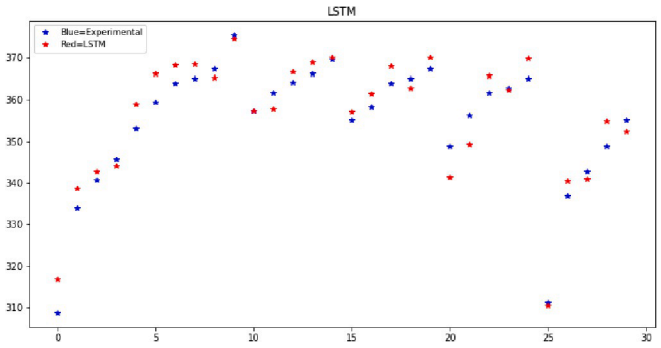

Fig. 8. Estimated h values obtained using LSTM.

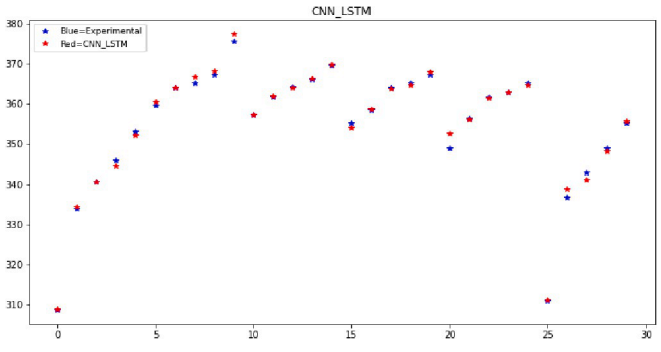

Fig. 9. Estimated h values obtained using CNN-LSTM.

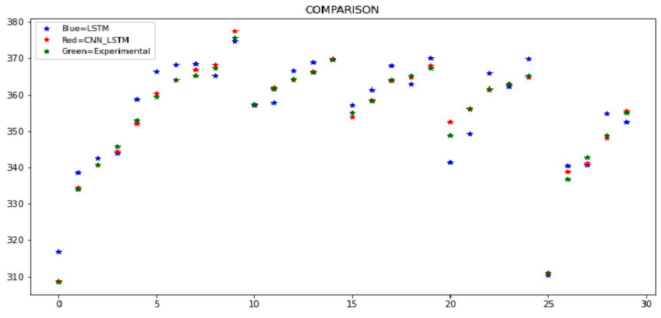

Fig. 10. Comparison of the experimental and estimated h values.

to increase heat transfer. It has been proven that the deep learning model created in our study has an accurate prediction feature as a result of its close approximation to the experimental results obtained in our research. The main purpose of using deep learning models in this study is;

- To analyze the accuracy of the experimental data obtained from the experimental study.

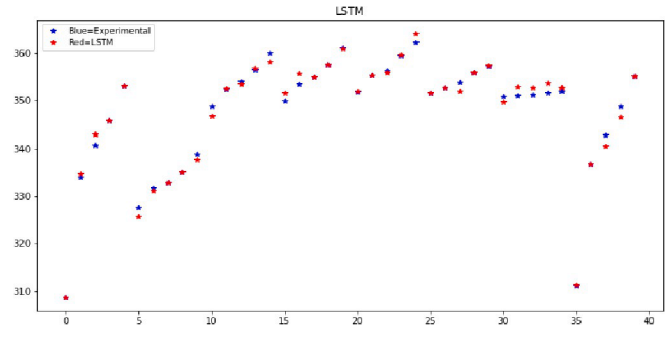

Fig. 11. Estimated h values obtained using LSTM for Magnetic Impact with Deep Learning.

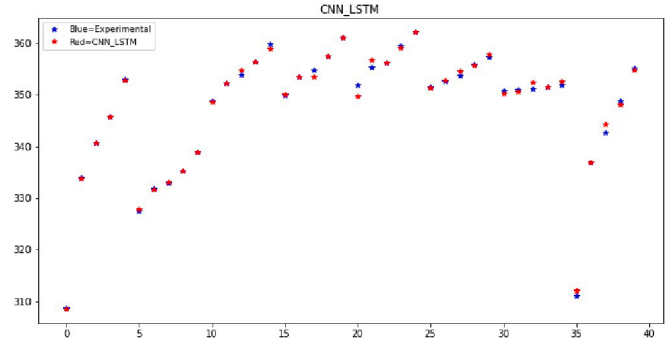

Fig. 12. Estimated h values obtained using CNN + LSTM for Magnetic Impact with Deep Learning.

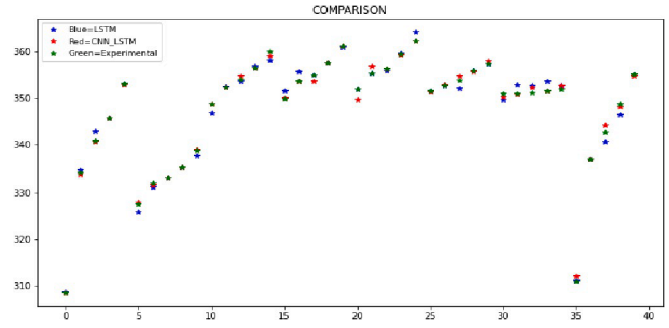

Fig. 13. Comparison of the experimental and estimated h values for Magnetic Impact with Deep Learning.

- To show that deep learning models can be used in the literature regarding such a study to be done.
- To prove that by developing deep learning models, time loss can be avoided in this field.

- For future studies, these data obtained from our research and verified by deep learning model should be taken into consideration.

Researchers will be able to avoid error analysis and repetition of experiments in experimental studies they plan to do with a structure similar to the one in this paper. Thus, the time spent on testing will be reduced. In future research, it has been observed that the required heat transfer coefficient results can be obtained by using this model for the desired Reynolds numbers in laminar flow for the researchers who will work in the experiment set and similar systems used in our study. For this reason, it has been concluded that the obtained model can prevent time losses that may occur as a result of careful examination by researchers who will work in this field.

Declaration of Competing Interest

The authors declare that they have no known competing financial interests or personal relationships that could have appeared to influence the work reported in this paper.

References

[1] J.P. Abraham, E.M. Sparrow, J.C.K. Tong, D.W. Bettenhausen, Sparrow Tong JCK, Bettenhause DW. Internal flows which transist from turbulent through intermittent to laminar, Int. J. Therm. Sci. 49 (2) (2010) 256–263.

[2] Maxwell J.C., A Treatise on Electricity and Magnetism, Clarendon Press, Oxford, UK, Second ed,1881.

[3] S. Gürmen, B. Ebin, Nanoparticles and Production Methods-1, Metall. J. 150 (2008) 31–38.

[4] Y. Xuan, Q. Li, Heat transfer enhancement of nanofluids, Int. J. Heat Fluid Flow 21 (1) (2000) 58–64.

[5] Choi S.U.S., Enhancing thermal conductivity of fluids with nanoparticles, The Proceedings of the 1995 ASME International Mechanical Engineering Congress and Exposition, San Francisco, USA, ASME, FED 231/MD 66, pp.99–105,1995.

[6] G. Colangelo, E. Favale, A. de Risi, D. Laforgia, Results of experimental investigations on the heat conductivity of nanofluids based on diathermic oil for high temperature applications, Appl. Energy 97 (2012) 828–833.

[7] J.A. Eastman, S.U.S. Choi, S. Li, W. Yu, L.J. Thompson, Anomalously increased effective thermal conductivity of ethylene glycol-based nanofluids containing copper nanoparticles, Appl. Phys. Lett. 78 (2001) 718–720.

[8] H. Chang, T.T. Tsung, Y.C. Yang, L.C. Chen, H.M. Lin, C.K. Lin, C.S. Jwo, Nanoparticle suspension preparation using the arc spray nanoparticle synthesis system combined with ultrasonic vibration and rotating electrode, Int. J. Adv. Manuf. Technol. 26 (5-6) (2005) 552–558.

[9] V. Kumar, A. Tiwari, S. Ghosh, Application of nanofluids in plate heat exchanger: a review, Energy Convers. Manage. 105 (2005) 1017–1036.

[10] C.T. Nguyen, F. Desgranges, R. Gilles, G. Nicolas, M. Thierry, S. Boucher, Temperature and particle-size dependent viscosity data for water-based nanofluids–hysteresis phenomenon, Int. J. Heat Fluid Flow 28 (6) (2007) 1492–1506.

[11] S. Yadav, S.K. Sahu, Heat transfer augmentation in double pipe water to air counter flow heat exchanger with helical surface disc turbulators, Chem. Eng. Process. Process Intensification 135 (2019) 120–132.

[12] J.S.V. Gonçalves, S.H. Santos, L.S. Leal, S. Junior, M.R.M.C. Santos, E. Longo, J.M. E. Matos, Experimental variables in the synthesis of anatase phase TiO_2 nanoparticles. 11th International Conference on Advanced Materials, Rio de janeiro Brazil, 2009.

[13] H. Xie, J. Wang, T. Xi, Y. Liu, Study on the thermal conductivity of SiC nanofluids, J. Chin. Ceram. Soc. 29 (4) (2001) 361–364.

[14] R. Suresh, V. Ponnuswamy, R. Mariappan, Effect of annealing temperature on the microstructural, optical and electrical properties of CeO2 nanoparticles by chemical precipitation method, Appl. Surf. Sci. 273 (2013) 457–464.

[15] M.-S. Liu, M. Ching-Cheng Lin, I.-T. Huang, C.-C. Wang, Enhancement of thermal conductivity with carbon nanotube for nanofluids, Int. Commun. Heat Mass Transfer 32 (9) (2005) 1202–1210.

[16] D. Wen, Y. Ding, Experimental investigation into convective heat transfer of nanofluids at the entrance region under laminar flow conditions, Int. J. Heat Mass Transf. 47 (24) (2004) 5181–5188.

[17] S.J. Kline, F.A. McClintock, Describing uncertainties in single-sample experiments, Mech. Eng. 75 (1953) 3–8.

[18] J.P. Holman, Experimental Methods for Engineers, 5th edition, Mc-Graw Hill Company, New York, 1989.

[19] E. Gil, J. Cortés, I. Iturriza, N. Ordás, XPS and SEM analysis of the surface of gas atomized powder precursor of ODS ferritic steels obtained through the STARS route, Appl. Surf. Sci. 427 (2018) 182–191.

[20] J.C. Miller, R. Serrato, J.M. Represas - Cardenas, G. Kundahl, The Handbook of Nanotechnology, John Wiley & Sons Inc, Hoboken, New Jersy, 2004.

[21] M. Kılıç, M. Yavuz, İ.H. Yılmaz, Numerical investigation of combined effect of nanofluids and impinging jets on heated surface, Int.. Adv. Res. Eng. J. 2 (1) (2018) 14–19.

[22] Juhi Patel, Kinnari Parekh, Effect of size and morphology on stability and thermal conductivity of ZnO nanofluid, J. Nanofluids 7 (2) (2018) 284–291.

[23] A.Y. Çengel, Practical Approach to Heat and Mass Transfer, McGraw Hill, 3rd Edition,, 2010, pp. 467–468.

[24] Neha Sharma, Reecha Sharma, Neeru Jindal, Machine learning and deep learning applications-a vision, Global Trans. Proc. 2 (1) (2021) 24–28, https://doi.org/10.1016/j.gltp.2021.01.004.

[25] Musab COŞKUN, Özal YILDIRIM, Ayşegül UÇAR, Yakup DEMIR, An overview of popular deep learning methods, Eur. J. Tech. 7 (2) (2017) 165–176.

[26] Coskun, M., Yildirim, O., Demir, Y., & Acharya, U. R., Efficient deep neural network model for classification of grasp types using sEMG signals. Journal of Ambient Intelligence and Humanized Computing, 1-14, 2021.

[27] A. Şeker, B. Diri, H.H. Balık, Derin öğrenme yöntemleri ve uygulamaları hakkında bir inceleme, Gazi Mühendislik Bilimleri Dergisi 3 (3) (2017) 47–64.

[28] T. Mikolov, A. Joulin, S. Chopra, M. Mathieu, A. Ranzato, Learning longer memory in recurrent neural networks, arXiv 1412 (2015) 7753.

[29] S. Hochreiter, J. Schmidhuber, Long short-term memory, Neural Comput. 9 (8) (1997) 1735–1780.

[30] Z. Jianfeng, M. Xia, C. Lijiang, Speech emotion recognition using deep 1D & 2D CNN LSTM networks, Biomed. Signal Process. Control 47 (2019) 312–323, https://doi.org/10.1016/j.bspc.2018.08.035.

[31] I. Touseef, Q. Shaima, The survey: Text generation models in deep learning, J. King Saud Univers. Comput. Inform. Sci. (2020), https://doi.org/10.1016/j.jksuci.2020.04.001.

[32] D. Mohit, Y. Rohit, M. Divya, B. Sonali, An improved RNN-LSTM based novel approach for sheet music generation, Procedia Comput. Sci. 171 (2020) 465–474, https://doi.org/10.1016/j.procs.2020.04.049.

[33] Emre Dandıl, Semih Karaca, Detection of pseudo brain tumors via stacked LSTM neural networks using MR spectroscopy signals, Biocybernet. Biomed. Eng. 41 (1) (2021) 173–195, https://doi.org/10.1016/j.bbe.2020.12.003.

[34] Yanzheng Lu, Hong Wang, Yangyang Qi, Hailong Xi, Evaluation of classification performance in human lower limb jump phases of signal correlation information and LSTM models, Biomed. Signal Process. Control 64 (2021) 102279, https://doi.org/10.1016/j.bspc.2020.102279.

[35] M. Kai-chao, H. Ting-ting, Y. Ye-qing, L. Hui, C. Peng, W. Bing, Z. Jun, Application of LSTM for short term fog forecasting based on meteorological elements, Neurocomputing 408 (2020) 285–291, https://doi.org/10.1016/j.neucom.2019.12.129.

[36] Sudhakaran Gajendran, Manjula D, Vijayan Sugumaran, Character level and word level embedding with bidirectional LSTM – Dynamic recurrent neural network for biomedical named entity recognition from literature, J. Biomed. Inform. 112 (2020) 103609, https://doi.org/10.1016/j.jbi.2020.103609.

[37] Shaojie Chen, Bo Lang, Hongyu Liu, Duokun Li, Chuan Gao, DNS covert channel detection method using the LSTM model, Comput. Sec. 104 (2021) 102095, https://doi.org/10.1016/j.cose.2020.102095.

[38] YiFei Li, Han Cao, Prediction for tourism flow based on LSTM neural network, Procedia Comput. Sci. 129 (2018) 277–283.

[39] Jiayu Qiu, Bin Wang, Changjun Zhou, Tao Song, Forecasting stock prices with long-short term memory neural network based on attention mechanism, PLoS ONE 15 (1) (2020) e0227222.

[40] G. Chniti, H. Bakir, H. Zaher, E-commerce time series forecasting using LSTM neural network and support vector regression, in: In Proceedings of the International Conference on Big Data and Internet of Thing, 2017, pp. 80–84.

[41] I.E. Livieris, E. Pintelas, N. Kiriakidou, S. Stavroyiannis, An advanced deep learning model for short-term forecasting U.S. natural gas price and movement. In Proceedings of the International Conference on Artificial Intelligence Applications and Innovations, 2020.

[42] Rui Yan, Jiaqiang Liao, Jie Yang, Wei Sun, Mingyue Nong, Feipeng Li, Multi-hour and multi-site air quality index forecasting in Beijing using CNN, LSTM, CNN-LSTM, and spatiotemporal clustering, Expert Syst. Appl. 169 (2021) 114513, https://doi.org/10.1016/j.eswa.2020.114513.

[43] Wei Yu, Huaqing Xie, Lifei Chen, Yang Li, Investigation of thermal conductivity and viscosity of ethylene glycol based ZnO nanofluid, Thermochim Acta 491 (1-2) (2009) 92–96.

[44] B. Souayeh, S. Bhattacharyya, N. Hdhiri, Alam M. Waqas, Heat and fluid flow analysis and ANN-Based prediction of a novel spring corrugated tape, Sustainability 13 (6) (2021) 3023.

[45] P.K. Kanti, K.V. Sharma, Z. Said, M. Jamei, K.M. Yashawantha, Experimental investigation on thermal conductivity of fly ash nanofluid and fly ash-Cu hybrid nanofluid: prediction and optimization via ANN and MGGP model, Part. Sci. Technol. 1–14 (2021).

[46] I.O. Alade, T.A. Oyehan, I.K. Popoola, S.O. Olatunji, A. Bagudu, Modeling thermal conductivity enhancement of metal and metallic oxide nanofluids using support vector regression, Adv. Powder Technol. 29 (1) (2018) 157–167.

[47] Abdolhossein Hemmati-Sarapardeh, Amir Varamesh, Maen M. Husein, Kunal Karan, On the evaluation of the viscosity of nanofluid systems: modeling and data assessment, Renew. Sustain. Energy Rev. 81 (2018) 313–329.

[48] Mohammad Hemmat Esfe, Afshin Tatar, Mohammad Reza Hassani Ahangar, Hossein Rostamian, A comparison of performance of several artificial intelligence methods for predicting the dynamic viscosity of TiO2/SAE 50 nano-lubricant, Phys. E 96 (2018) 85–93.

[49] Masoud Afrand, Afshin Ahmadi Nadooshan, Mohsen Hassani, Hooman Yarmand, M. Dahari, Predicting the viscosity of multi-walled carbon nanotubes/water

nanofluid by developing an optimal artificial neural network based on experimental data, Int. Commun. Heat Mass Transfer 77 (2016) 49–53.

[50] Mohammad Hossein Ahmadi, Mohammad Ali Ahmadi, Mohammad Alhuyi Nazari, Omid Mahian, Roghayeh Ghasempour, A proposed model to predict thermal conductivity ratio of Al $_{2}$ O 3/EG nanofluid by applying least squares support vector machine (LSSVM) and genetic algorithm as a connectionist approach, J. Therm. Anal. Calorim. 135 (1) (2019) 271–281.

[51] M.H. Ahmadi, A. Tatar, P. Seifaddini, M. Ghazvini, R. Ghasempour, M.A. Sheremet, Thermal conductivity and dynamic viscosity modeling of Fe_2O_3/water nanofluid by applying various connectionist approaches, Numer. Heat Trans. Part A Appl. 74 (6) (2018) 1301–1322.